

## Temperature dependence of optical anisotropy of birefringent porous silicon

Kohei Nishida,<sup>1</sup> Minoru Fujii,<sup>1,a)</sup> Shinji Hayashi,<sup>1</sup> and Joachim Diener<sup>2</sup>

<sup>1</sup>Department of Electrical and Electronic Engineering, Graduate School of Engineering, Kobe University, Rokkodai, Nada, Kobe 657-8501, Japan

<sup>2</sup>Physik-Department E16, Technische Universität München, D-85747 Garching, Germany

(Received 21 January 2010; accepted 23 May 2010; published online 14 June 2010)

Temperature dependence of the in-plane optical anisotropy of birefringent porous Si produced from a (110) Si wafer is studied. The anisotropy of refractive indices in the [001] and  $[1\bar{1}0]$  directions increased about 0.3% when the temperature rose from 30 to 100 °C. The effective medium approximation could reproduce the experimental result in the low temperature range, while discrepancy appeared at high temperatures. The discrepancy suggests that the structural anisotropy of porous Si starts to relax at relatively low temperatures. © 2010 American Institute of Physics. [doi:10.1063/1.3453449]

Nanostructuring is a fast growing field in modern solid-state physics. It is well-known that a three-dimensional network of Si nanowire skeletons can be produced by electrochemical etching of Si wafers (porous silicon: PSi). The sizes of nanowires and pores are usually much smaller than the wavelength of visible light, and thus PSi can be regarded as a uniform dielectric material. This concept is a basis of the variety of dielectric PSi structures like microcavities,<sup>1</sup> distributed Bragg reflectors,<sup>2</sup> aperiodic multilayers,<sup>3,4</sup> and waveguides.<sup>5</sup> These optical components operate in a wide wavelength range typically from 800 nm to 5  $\mu\text{m}$ .

When PSi is produced from a (100) Si wafer, the nanowires and pores are aligned in the growth direction. This results in isotropic effective dielectric constants in the plane perpendicular to the growth direction. On the other hand, when PSi is produced from a wafer with lower symmetry, the direction of pores is not necessarily in the direction of current flow. For example, in the case of PSi produced from (110) wafers, the pores proceed in equivalent  $\langle 100 \rangle$  directions. This results in anisotropy of the effective refractive indices in the [001] and  $[1\bar{1}0]$  directions (in-plane birefringence).<sup>6</sup> The degree of optical anisotropy ( $\Delta n = n_{[1\bar{1}0]} - n_{[001]}$ ) reaches as large as 0.17,<sup>7</sup> which is comparable to that of calcite. The advantage of birefringent PSi to produce optical components is that the refractive indices in the [001] and  $[1\bar{1}0]$  directions can be controlled by the etching current density. By precisely controlling the etching current, a variety of polarizing elements such as polarizers and dichroic mirrors are produced.<sup>7,8</sup>

In this work, we study temperature dependence of the optical anisotropy of birefringent PSi. The information is indispensable to design polarizing elements from birefringent PSi and to guarantee the operation in a wide temperature range. We produce an optical wave-plate from a birefringent PSi and study the temperature dependence of the characteristic wavelengths. By analyzing the results, temperature dependence of  $\Delta n$  is estimated and the origin of the temperature dependence is discussed.

PSi layers were produced by electrochemical etching of (110) oriented p<sup>+</sup> Si wafers (1–5 m $\Omega$  cm). Etching was performed at room temperature in a solution of 1:1 by volume mixture of HF (46 wt % in water) and ethanol. The etching-current density was 60 mA/cm<sup>2</sup> and the porosity of the layer was about 0.7. The layer thickness was about 98  $\mu\text{m}$ . During the etching process, several etch-stop steps of zero current were inserted to recover the HF concentration at the etching front. At the end of the etching process, a high current pulse (400 mA/cm<sup>2</sup>, 1.6 s) was applied to detach PSi structures from the substrate. The free-standing layer was then annealed in air at 600 °C for 3 min. The annealing process stabilizes the optical property.

The optical anisotropy of the refractive index was determined by the analysis of the polarization state of light transmitted through a sample. Transmittance spectra were measured by a spectrophotometer (Shimadzu UV-3101PC) over the spectral range of 1200 to 1800 nm with the spectral resolution of 0.2 nm. The experimental setup is shown in Fig. 1. The incident light was linearly polarized by a Glan-Thompson prism. Polarization of the incident light ( $I_0$ ) was aligned at 45° to the [001] and  $[1\bar{1}0]$  directions of the layer. Spectra with the polarization direction either perpendicular ( $I_{\perp}$ ) or parallel ( $I_{\parallel}$ ) to that of the incident light were recorded. Figure 2(a) shows the ratio of  $I_{\perp}$  and  $I_{\parallel}$  ( $I_{\perp}/I_{\parallel}$ ) measured at 30 °C. The temperature is changed from 30 to 100 °C by using silicone rubber heater attached on the sample stage. The temperature was monitored by a thermocouple placed close to the sample.

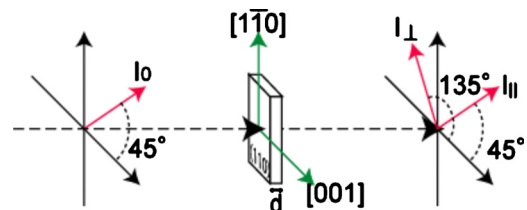


FIG. 1. (Color online) Experimental setup for the measurement of  $I_{\perp}/I_{\parallel}$ .  $I_{\perp}$  and  $I_{\parallel}$  are the intensities of the transmitted light whose polarization directions are perpendicular and parallel, respectively, to that of the incident light.

<sup>a)</sup>Electronic mail: fujii@eedept.kobe-u.ac.jp.

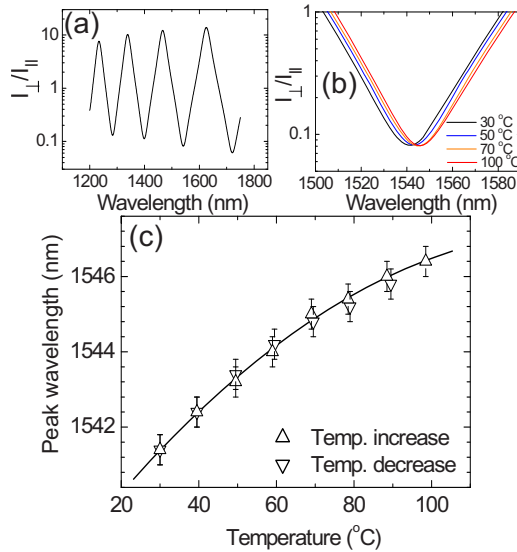


FIG. 2. (Color online) (a)  $I_{\perp}/I_{\parallel}$  measured at 30 °C. (b) Expansion of (a) around 1540 nm at 30, 50, 70, and 100 °C. (c) Temperature dependence of the peak wavelength around 1540 nm. Triangles and reverse triangles represent experimental data obtained when the temperature increases and decreases, respectively. Solid curve is a guide to the eyes.

While light travels through the optically anisotropic layer, its components polarized along  $[001]$  and  $[1\bar{1}0]$  directions experience a phase shift  $\Delta\phi$ . The minima (maxima) in Fig. 2(a) corresponds to even (odd) orders of  $\pi$  phase shift. Figure 2(b) shows the expansion of Fig. 2(a) at different temperatures. We can see the shift in the minima to longer wavelength by the increase in the temperature. The shift indicates that  $\Delta n$  depends on temperature. In Fig. 3, the minima in Fig. 2(b) is plotted as a function of the temperature. The triangles and reverse triangles represent experimental data, while the solid line is the results of a least-square fitting of the data. The triangle corresponds to the data taken when the temperature increases, while the reverse triangle to that when the temperature decreases. No hysteresis of the peak wavelength is seen in the temperature cycles. We repeated the temperature rising and lowering cycles several times, and no degradation of the optical properties was seen when the maximum temperature was 100 °C. The error bars represent the wavelength accuracy of the spectrophotometer.

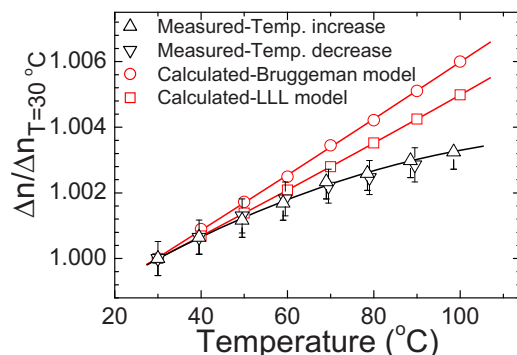


FIG. 3. (Color online) Temperature dependence of the degree of birefringence around 1540 nm normalized to that at 30 °C. Triangles ( $\Delta$ ) and reverse triangles ( $\nabla$ ) represent experimental data, while squares ( $\square$ ) and circles ( $\circ$ ) represent calculated values based on Bruggeman and LLL models, respectively. Solid curves are guides to the eyes.

The temperature dependence of  $\Delta n$  is derived from the shift in the  $I_{\perp}/I_{\parallel}$  minima by using

$$\Delta n = \frac{\lambda}{2\pi d} \Delta\phi, \quad (1)$$

where  $d$  is the thickness of the film.<sup>6</sup> In Fig. 3,  $\Delta n(T)$  normalized to that at 30 °C [ $\Delta n(30 \text{ °C})$ ] is plotted as a function of temperature ( $\Delta$  and  $\nabla$ ).  $\Delta n$  increases about 0.3% when the temperature is changed from 30 to 100 °C.

In order to explain the origin of the temperature dependence of the anisotropy, we try to calculate it based on the effective medium approximation (EMA) by using the refractive indices of bulk Si crystal and air. Among many kinds of EMA models,<sup>9</sup> Bruggeman and Landau–Lifshitz and Looyenga (LLL) models have widely been applied to PSi.<sup>10</sup> In general, the Bruggeman model is more suitable when the porosity is below 0.7, while the LLL model is more suitable above 0.7.<sup>10</sup> In this work, the porosity is around 0.7. Therefore, we will calculate the refractive indices by using the two models. The Bruggeman model is expressed as<sup>11</sup>

$$\sum_i f_i \left( \frac{\varepsilon_i - \varepsilon_{av}}{\varepsilon_i + 2\varepsilon_{av}} \right) = 0, \quad (2)$$

while the LLL model is expressed as<sup>9</sup>

$$\varepsilon_{av}^{1/3} = \sum_i f_i \varepsilon_i^{1/3}, \quad (3)$$

where  $f_i$  is the volume fraction of the  $i$ th medium (either Si or air),  $\varepsilon_i$  is its dielectric constant, and  $\varepsilon_{av}$  is the dielectric constant of the mixture.

To apply the Bruggeman and LLL models to the birefringent PSi, we introduce two effective filling factors,  $f_{[001]}$  and  $f_{[1\bar{1}0]}$ , along the  $[001]$  and  $[1\bar{1}0]$  directions, respectively.<sup>12</sup> First, at a specific wavelength ( $\lambda \sim 2000$  nm), refractive indices,  $n_{[001]}$  and  $n_{[1\bar{1}0]}$ , are determined from the interference fringes of the transmittance spectra. From the  $n_{[001]}$  and  $n_{[1\bar{1}0]}$ ,  $f_{[001]}$  and  $f_{[1\bar{1}0]}$ , respectively, are calculated by using the Bruggeman and LLL models under the assumption that PSi is a mixture of crystalline Si and air. The refractive index of crystalline Si ( $n_{Si}$ ) is taken from a literature.<sup>13</sup> The obtained  $f_{[001]}$  and  $f_{[1\bar{1}0]}$  are then used to calculate the wavelength dependence of  $n_{[001]}$  and  $n_{[1\bar{1}0]}$ .

To calculate the temperature dependence of  $\Delta n$ , we assume that  $n_{Si}$  and  $n_{air}$  are temperature dependent, while  $f_{[001]}$  and  $f_{[1\bar{1}0]}$  are temperature independent. Unfortunately, the literature values of  $dn_{Si}/dT$  is scattered in a wide range.<sup>14,15</sup> In this work, we use the  $dn_{Si}/dT$  values reported in Ref. 15;  $dn/dT = 8.61 \times 10^{-5} + 3.63 \times 10^{-7} \times T - 2.07 \times 10^{-10} \times T^2$  (K<sup>-1</sup>). The  $dn_{air}/dT$  value is taken from the literature ( $-10^{-6}$  K<sup>-1</sup>).<sup>16</sup>

The calculated temperature dependence of  $\Delta n$  for Bruggeman and LLL models is shown in Fig. 3 by squares and circles, respectively. They increase almost linearly with temperature. The LLL model exhibits smaller values than the Bruggeman model and has better agreement with the experimental results. At low temperatures ( $<50$  °C), the agreement between experimental and calculated values (LLL model) is reasonable. The discrepancy appears above 50 °C and becomes significant at higher temperatures. The measured value starts to saturate around 50 °C, while the calcu-

lated value continues to increase and is twice as large as that of the measured one at 100 °C. Therefore, the temperature dependence of the optical anisotropy of birefringent PSi is much smaller than that expected from the refractive index of bulk Si crystal. The temperature insensitiveness of  $\Delta n$  is a great advantage when we design and produce temperature-stable polarizing elements from birefringent PSi.

At present, the reason for the discrepancy between measured and calculated temperature dependence of  $\Delta n$  is not clear. One of the possible explanations is that refractive index of Si nanowires constructing PSi is changed from that of bulk Si crystal because of the small size and the resultant large surface to volume ratio. Another more plausible explanation is that the structural anisotropy of PSi is relaxed at high temperatures and the structure becomes more isotropic. In this work, the highest temperature is limited to 100 °C because of the instrumental limitation. In this temperature range, the detection of the structural change is considered to be very difficult. It is very interesting to study how the structural anisotropy of PSi is modified and how it affects the optical anisotropy at higher temperatures.

In conclusion, we studied the temperature dependence of the optical anisotropy of birefringent PSi and showed that it slightly depends on the temperature, i.e.,  $\Delta n$  increases 0.3% from 30 to 100 °C. The analysis of the data by the Bruggeman and LLL models revealed that the temperature dependence cannot be fully explained when the temperature dependence of the refractive index of bulk Si crystal is considered, i.e., temperature dependence of  $\Delta n$  is smaller

than that expected from the EMAs. This may suggest that the structure of PSi changes by temperature. The present results suggest that the properties of optical components made from birefringent PSi is temperature stable and can be used at least up to 100 °C.

- <sup>1</sup>V. Mulloni and L. Pavesi, *Appl. Phys. Lett.* **76**, 2523 (2000).
- <sup>2</sup>G. Vincent, *Appl. Phys. Lett.* **64**, 2367 (1994).
- <sup>3</sup>L. Moretti, I. Rea, L. Rotiroli, I. Rendina, G. Abbate, A. Marino, and L. De Stefano, *Opt. Express* **14**, 6264 (2006).
- <sup>4</sup>V. Agarwal, M. E. Mora-Ramos, and B. Alvarado-Tenorio, *Photonics Nanostruct. Fundam. Appl.* **7**, 63 (2009).
- <sup>5</sup>H. Arrand, M. T. Benson, T. Anada, M. Krueger, M. G. Berger, R. Aren-Fischer, H. G. Munder, H. Luth, A. Loni, and R. J. Bozeat, *Integrated Photonics Research, OSA Technical Digest Series Technical Digest* **6**, 311 (1996).
- <sup>6</sup>N. Künzner, D. Kovalev, J. Diener, E. Gross, V. Y. Timoshenko, G. Polisski, F. Koch, and M. Fujii, *Opt. Lett.* **26**, 1265 (2001).
- <sup>7</sup>N. Ishikura, M. Fujii, K. Nishida, S. Hayashi, and J. Diener, *Opt. Express* **16**, 15531 (2008).
- <sup>8</sup>J. Diener, N. Kunzer, E. Gross, D. Kovalev, and M. Fujii, *Opt. Lett.* **29**, 195 (2004).
- <sup>9</sup>J. E. Spanier and I. P. Herman, *Phys. Rev. B* **61**, 10437 (2000).
- <sup>10</sup>L. Moretti, L. De Stefano, A. M. Rossi, and I. Rendina, *Appl. Phys. Lett.* **86**, 061107 (2005).
- <sup>11</sup>D. A. G. Bruggeman, *Ann. Phys.* **416**, 636 (1935).
- <sup>12</sup>P. A. Snow, E. K. Squire, P. S. J. Russell, and L. T. Canham, *J. Appl. Phys.* **86**, 1781 (1999).
- <sup>13</sup>*Handbook of Optical Constants of Solids*, edited by E. D. Palik (Academic, New York, 1985).
- <sup>14</sup>G. E. Jellison and H. H. Burke, *J. Appl. Phys.* **60**, 841 (1986).
- <sup>15</sup>F. G. Della Corte, M. E. Montefusco, L. Moretti, I. Rendina, and G. Cocorullo, *J. Appl. Phys.* **88**, 7115 (2000).
- <sup>16</sup>J. W. Goodman, *Statistical Optics* (Wiley, New York, 1985).